

---

# On the Implicit Bias Towards Depth Minimization in Deep Neural Networks

---

**Tomer Galanti**

CBMM

Massachusetts Institute of Technology

MA, USA

galanti@mit.edu

**Liane Galanti**

School of Computer Science

Tel Aviv University

Israel

lianegalanti@mail.tau.ac.il

## Abstract

We study the implicit bias of stochastic gradient descent to favor low-depth solutions when training deep neural networks. Recent results in the literature suggest that penultimate layer representations learned by a classifier over multiple classes exhibit a clustering property, called neural collapse. First, we empirically show that neural collapse generally strengthens when increasing the number of layers. In addition, we demonstrate that neural collapse extends beyond the penultimate layer and emerges in intermediate layers as well, making the higher layers essentially redundant. We characterize the notion of effective depth which measures the minimal layer that enjoys neural collapse. In this regard, we hypothesize and empirically show that gradient descent implicitly selects neural networks of small effective depths. Finally, we theoretically and empirically show that the effective depth of a trained neural network monotonically increases when training with extended portions of random labels and connect it with generalization.

## 1 Introduction

Deep learning systems have steadily advanced the state of the art in a wide variety of benchmarks, demonstrating impressive performance in tasks ranging from image classification [Taigman et al., 2014, Zhai et al., 2021], language processing [Devlin et al., 2019, Brown et al., 2020], open-ended environments [Silver et al., 2016, Arulkumaran et al., 2019], to coding [Chen et al., 2021].

A central aspect that enables the success of these systems is the ability to train deep models instead of wide shallow ones [He et al., 2016]. Intuitively, a neural network is decomposed into hierarchical representations from raw data to high-level, more abstract features. While training deeper neural networks repetitively achieves superior performance against their shallow counterparts He et al. [2015], Wang et al. [2022], an understanding of the role of depth in representation learning is still lacking.

Multiple contributions (e.g., Poggio et al. [2020], Safran et al. [2021], Eldan and Shamir [2016]) studied the role of depth from the view point of approximation theory and expressivity. These works suggest that in certain cases it requires less parameters in order to approximate a given smooth target function using deeper networks. While these papers demonstrate superior approximation guarantees for deeper networks, it is typically possible to fit the training data (and test data) even by using a shallow fully-connected network. In addition, these papers measure the success of neural networks as the best approximation a given architecture provides for a given target function. Therefore, these papers do not take into account on the specific functionalities captured by different layers of the trained model.

As an attempt to understand the training dynamics of neural networks, another line of work considers the training dynamics of neural networks of very large widths [Jacot et al., 2018]. In [Lee et al., 2019] they showed that under certain conditions, training wide shallow neural networks with gradient decent converges to a solution of kernel regression with the neural tangent kernel (NTK). However, this result makes several unrealistic assumptions that give rise to training dynamics that abstain from learning representations. These assumptions include: large widths, incorporating a non-standard initialization procedure and the absence of batch normalization layers [Jacot et al., 2019].

Recently, Papyan et al. [2020] suggested a different perspective for understanding the representations learned by neural networks in a standard setting (e.g., with batch normalization, standard initialization, etc') in the lens of neural collapse. Informally, neural collapse (NC) identifies training dynamics of deep networks for standard classification tasks, where the features of the penultimate layer associated with training samples belonging to the same class tend to concentrate around their means. Specifically, Papyan et al. [2020] observed that the ratio of the within-class variances and the distances between the class means tends to zero, especially at the terminal stage when training proceeds beyond perfectly fitting the training labels. They also noticed that asymptotically the class-means (centered at their global mean) are not only linearly separable, but are actually maximally distant and located on a sphere centered at the origin up to scaling (they form a simplex equiangular tight frame). Furthermore, it has also been observed that the features are *nearest class-center separable*, meaning that a nearest class-center classifier on top of the features is able to perfectly distinguish between the classes. In addition to that, it has been shown that the behavior of the last-layer classifier (operating on the features) converges to that of the nearest class-center decision rule. Since neural collapse deals with a setting in which the within-class variability of the penultimate layer is small, we can intuitively say that the classification is essentially already done at the penultimate layer.

**Contributions.** In this work we suggest a new perspective on understanding the role of depth in deep learning. We observe that *SGD training of deep neural networks exhibits an implicit bias that favors solutions of minimal depth for achieving nearest class-center classification*.

The central contributions in this work are:

- We empirically show that in contrast to original predictions, neural collapse does not necessarily happen at the stage of training when the network perfectly fits the data. Instead, we show that it emerges only if the network is sufficiently deep. In addition, we show that neural collapse generally improves when increasing the network's depth.
- We characterize and study the *effective depth* of neural networks that measures the lowest layer's features that are NCC separable. We empirically show that when training a neural network, SGD favors solutions of small effective depths. Specifically, the feature embeddings of layers above a certain minimal depth of the neural network are NCC separable.
- We empirically show that the effective depth of neural networks increases when trained with extended portions of corrupted labels and we theoretically support its connection with generalization.
- We empirically show that NCC classifiers corresponding to intermediate layers of achieve better test performance in comparison with the original trained classifier, when trained with noisy labels.

**Organization.** The rest of the paper is organized as follows: Some additional related work is discussed in Section 1.1. The problem setting is introduced in Section 2. Neural collapse, the effective depths of neural networks and their relation with generalization are presented in Section 3. Experiments are presented in Section 4, and conclusions are drawn in Section 5.

## 1.1 Additional Related Work

**Neural collapse and generalization.** The relationship between neural collapse and generalization has been addressed multiple times in the literature. In [Galanti et al., 2022] they theoretically and empirically studied the conditions for neural collapse to generalize from train samples, to test samples and new classes and its implications on transfer learning. For instance, they showed that in the regime of neural collapse, if the number of training samples tends to infinity, we should encounter neural collapse on the test samples as well. This raises the following question: *does neural collapse indicate whether the network generalizes?* As an argument against it, Mixon et al. [2020] provided empirical

evidence that neural collapse emerges when training the network with random labels. Namely, the presence of neural collapse itself does not indicate whether the network generalizes or not.

To study the relation between neural collapse and generalization, we make the following set of observations. First, we observe that the degree of neural collapse (on the training samples) generally improves when increasing the number of layers. Second, by extending the experiment of Mixon et al. [2020], we observe that the degree of neural collapse when training with the correct labels is higher than the neural collapse achieved when a subset of the labels are corrupted. Furthermore, we show that the effective depth increases when training neural networks with extended portions of corrupted labels. Therefore, we conclude that the presence of neural collapse itself only weakly indicates whether the network generalizes or not. Instead, we propose the effective depth of networks as a better indicator whether generalization is evident or not.

**Neural collapse in intermediate layers.** While the original motivation in Popyan et al. [2020] was to study the variability collapse of the penultimate layer and the convergence of the network’s last layer to a nearest class-center classifier, it is tempting to understand whether this behaviour also extends below the network’s penultimate layer. For the purpose of studying the relationship between neural collapse and transferability, Galanti et al. [2022] investigated the emergence of neural collapse in intermediate layers. Specifically, they compared the degree of variability collapse in the second-to-last embedding layer of a residual network with the variability collapse in the penultimate layer. This paper observed that while we can see a similar clustering behaviour as in the penultimate layer, the extent is lower. In Ben-Shaul and Dekel [2022] they consider the emergence of neural collapse in intermediate layers of neural networks by looking at the nearest class-center classification error of various layers of the networks. However, none of these papers identified the minimal-depth principle that we characterize and study in this work.

## 2 Problem Setup

We consider the problem of training a model for a standard multi-class classification. Formally, the target task is defined by a distribution  $P$  over samples  $(x, y) \in \mathcal{X} \times \mathcal{Y}_C$ , where  $\mathcal{X} \subset \mathbb{R}^d$  is the instance space, and  $\mathcal{Y}_C$  is a label space with cardinality  $C$ . To simplify the presentation, we use one-hot encoding for the label space, that is, the labels are represented by the unit vectors in  $\mathbb{R}^C$ , and  $\mathcal{Y}_C = \{e_c : c = 1, \dots, C\}$  where  $e_c \in \mathbb{R}^C$  is the  $c$ th standard unit vector in  $\mathbb{R}^C$ ; with a slight abuse of notation, sometimes we will also write  $y = c$  instead of  $y = e_c$ . For a pair  $(x, y)$  distributed by  $P$ , we denote by  $P_c$  the class conditional distribution of  $x$  given  $y = c$  (i.e.,  $P_c(\cdot) = \mathbb{P}[x \in \cdot \mid y = c]$ ).

A classifier  $h_W : \mathcal{X} \rightarrow \mathbb{R}^C$  assigns a *soft* label to an input point  $x \in \mathcal{X}$ , and its performance on the distribution  $P$  is measured by the risk

$$L_P(h_W) = \mathbb{E}_{(x, y(x)) \sim P} [\ell(h_W(x), y(x))], \quad (1)$$

where  $\ell : \mathbb{R}^C \times \mathcal{Y}_C \rightarrow [0, \infty)$  is a non-negative loss function (e.g.,  $L_2$  or cross-entropy losses). For simplicity, sometimes we will omit writing  $W$  in the subscript of  $h$ .

We typically do not have direct access to the full population distribution  $P$ . Therefore, we typically aim to learn a classifier,  $h$ , from some balanced training data  $S = \{(x_i, y_i)\}_{i=1}^m = \bigcup_{c=1}^C S_c = \bigcup_{c=1}^C \{(x_{ci}, y_{ci})\}_{i=1}^{m_0} \sim P_B(m)$  of  $m = C \cdot m_0$  samples consisting  $m_0$  independent and identically distributed (i.i.d.) samples drawn from  $P_c$  for each  $c \in [C]$ . Specifically, we intend to find  $W$  that minimizes the empirical risk

$$L_S(h_W) = \frac{1}{m} \sum_{i=1}^m \ell(h_W(x_i), y_i). \quad (2)$$

Finally, the performance of the trained model is evaluated using the train and test error rates, which are computed as follows:  $\text{err}_S(h_W) = \sum_{i=1}^m \ell(h_W(x_i), y_i)$  and  $\text{err}_P(h_W) = \mathbb{E}_{(x, y) \sim P} [\ell(h_W(x), y)]$ .

**Neural Networks.** In this work, the classifier  $h_W$  is implemented as a neural network, decomposed into a set of parametric layers. Formally, we write  $h_W := e_{W_e} \circ f_{W_f}^L := e_{W_e} \circ g_{W_L}^L \circ \dots \circ g_{W_1}^1$ , where  $g_{W_i}^i \in \{g' : \mathbb{R}^{p_i} \rightarrow \mathbb{R}^{p_{i+1}}\}$  are parametric functions and  $e_{W_e} \in \{e' : \mathbb{R}^{p_{L+1}} \rightarrow \mathbb{R}^C\}$  is a linear function. For example,  $g_{W_i}^i$  could be a standard layer  $g_{W_i}^i(z) = \sigma(W_i \cdot z)$ , a residual block  $g_{W_i}^i(z) = z + W_i^2 \sigma(W_i^1 z)$  or a pooling layer. Here,  $\sigma$  is an element-wise ReLU activation function.

We denote the  $i$ th layer of the neural network as  $f^i = g^i \circ \dots \circ g^1$ , for  $i \leq L$ . With a slight abuse of notations, sometimes we will omit specifying the sub-scripted weights, e.g.,  $h = h_W$  and  $f^i = f_{W_f}^i$ .

**Optimization.** In this work, we consider optimizing our model using stochastic gradient decent (SGD). We aim at minimizing the regularized empirical risk  $L_S^\lambda(h) = L_S(h) + \lambda\|W\|_2^2$  by applying SGD for a certain number of iterations  $T$  with coefficient  $\lambda > 0$ . Namely, we initialize the weights  $W_0 = \gamma$  of  $h$  using a standard initialization procedure and at each iteration, we update  $W_{t+1} \leftarrow W_t - \mu_t \nabla_W L_{\tilde{S}}(h_t)$ , where  $\mu_t > 0$  is the learning rate at the  $t$ 'th iteration and the subset  $\tilde{S} \subset S$  of size  $B$  is selected uniformly at random. Throughout the paper, we denote by  $h_S^\gamma$  the output of the learning algorithm starting from the initialization  $W_0 = \gamma$ . When  $\gamma$  is irrelevant or obvious from context, we will simply write  $h_S^\gamma = h_S = e_S \circ f_S$ .

**Notations.** Throughout the paper, we use the following notations. For an integer  $k \geq 1$ ,  $[k] = \{1, \dots, k\}$ . For any real vector  $z$ ,  $\|z\|$  denotes its Euclidean norm. We denote by  $\mu_u(Q) = \mathbb{E}_{x \sim Q}[u(x)]$  and by  $\text{Var}_u(Q) = \mathbb{E}_{x \sim Q}[\|u(x) - \mu_u(Q)\|^2]$  the mean and variance of  $u(x)$  for  $x \sim Q$ . For a finite set  $A$ , we denote by  $U[A]$  the uniform distribution over  $A$ . We denote by  $\mathbb{I} : \{\text{True, False}\} \rightarrow \{0, 1\}$  the indicator function. For a given distribution  $P$  over  $\mathcal{X}$  and a measurable function  $f : \mathcal{X} \rightarrow \mathcal{X}'$ , we denote the distribution of  $f(x)$  by  $f \circ P$ . Let  $U = \{y_i\}_{i=1}^m$  be a set of labels  $y_i \in [C]$ . We denote  $D(U) = (p_1, \dots, p_C)$ , with  $p_c = \frac{1}{m} \sum_{i=1}^m \mathbb{I}[y_i = c]$ .

### 3 Neural Collapse and Generalization

In this section we theoretically explore the relationship between neural collapse and generalization. We begin by formally introducing neural collapse, NCC separability along with the effective depth of neural networks. Then, we connect these notions with the test-time performance of neural networks.

#### 3.1 Neural Collapse

As mentioned in Section 1, neural collapse considers training dynamics of deep networks for standard classification tasks, in which the features of the penultimate layer associated with training samples belonging to the same class tend to concentrate around their class means. In this paper, we focus on the class-features variance collapse (NC1) and the nearest class-center classifier simplification (NC4) properties of neural collapse.

To evaluate NC1, we follow the evaluation process suggested by Galanti et al. [2022], that works with a slightly different variation of within-class variation collapse, which is related with the clusterability of the sample feature vectors. For a feature map  $f : \mathbb{R}^d \rightarrow \mathbb{R}^p$  and two (class-conditional) distributions<sup>1</sup>  $Q_1, Q_2$  over  $\mathcal{X} \subset \mathbb{R}^d$ , we define their *class-distance normalized variance* (CDNV) to be

$$V_f(Q_1, Q_2) = \frac{\text{Var}_f(Q_1) + \text{Var}_f(Q_2)}{2\|\mu_f(Q_1) - \mu_f(Q_2)\|^2}.$$

The definition of Galanti et al. [2022] for *neural collapse* (at training) asserts that

$$\lim_{t \rightarrow \infty} \text{Avg}_{i \neq j \in [l]} [V_{f^{(t)}}(S_i, S_j)] = 0,$$

where  $f^{(t)}$  is the value of the penultimate layer  $f = g^L \circ \dots \circ g^1$  of the neural network  $h = e \circ f$  at iteration  $t$  of the training. As shown empirically in Galanti et al. [2022], this definition is essentially the same as that of Papyan et al. [2020].

The nearest class-center classifier simplification property asserts that, during training, the feature embeddings in the penultimate layer become separable and classifier  $h$  itself converges to the ‘nearest class-center classifier’,  $\hat{h}$ . Formally, suppose we have a dataset  $S = \{(x_i, y_i)\}_{i=1}^m = \bigcup_{c=1}^C S_c$  of samples and a feature map  $f : \mathbb{R}^d \rightarrow \mathbb{R}^p$ , we say that the features of  $f$  are NCC separable, if

$$\forall j \in [m] : \hat{h}(x_j) = \arg \min_{c \in [C]} \|f(x_j) - \mu_f(S_c)\| = y_j. \quad (3)$$

As additional measures of collapse of a given layer, we also use the NCC train and test error rates,  $\text{err}_S(\hat{h})$  and  $\text{err}_P(\hat{h})$ , which are the error rates of  $\hat{h}(x) = \arg \min_{c \in [C]} \|f(x) - \mu_f(S_c)\|$ . As shown in [Galanti et al., 2022], the NCC error rate can be upper bounded in terms of the CNDV. However, the NCC error can be zero in cases where the CNDV would be larger than zero.

<sup>1</sup>The definition can be extended to finite sets  $S_1, S_2 \subset \mathcal{X}$  by defining  $V_f(S_1, S_2) = V_f(U[S_1], U[S_2])$ .

### 3.2 Effective Depths and Generalization

In this section we study the effective depths of neural networks and its connection with generalization. We argue that neural networks trained for standard classification exhibit an implicit bias towards depth minimization. This is summarized in the following observation.

**Observation 1** (Minimal depth hypothesis). *Suppose we have a dataset  $S$ . There exists an integer  $L_0 \geq 1$ , such that, if we train a model  $h = e \circ f^L$  of any depth  $L \geq L_0$  for classification on  $S$  using SGD, the learned features  $f^l$  become NCC separable for all  $l \in \{L_0, \dots, L\}$ .*

In particular, if the  $L_0$ 'th layer of  $f_L$  exhibits NCC separability, we could correctly classify the samples already in the  $L_0$ 'th layer of  $f_L$  using a linear classifier (i.e., the nearest class-center classifier). Therefore, its depth is effectively upper bounded by  $L_0$ . The notion of effective depth is formally defined as follows.

**Definition 1** (Effective depth). *Suppose we have a dataset  $S$ , a neural network  $h = e \circ g^L \circ \dots \circ g^1$  with  $g^1 : \mathbb{R}^n \rightarrow \mathbb{R}^{p_2}$ ,  $g^i : \mathbb{R}^{p_i} \rightarrow \mathbb{R}^{p_{i+1}}$  and linear classifier  $e : \mathbb{R}^{p_{L+1}} \rightarrow \mathbb{R}^C$ . The empirical effective depth  $d_S(h)$  of  $h$  is the minimal value  $i \in [L]$ , such that,  $\hat{h}_i(x_j) = \arg \min_{c \in [C]} \|f_i(x_j) - \mu_{f_i}(S_c)\| = y_j$  for all  $j \in [m]$  (and  $d_S(h) = \infty$  otherwise).*

While our empirical observations in Sec. 4 demonstrate that the optimizer tends to learn neural networks of low-depths, it is not necessarily the lowest depth that allows NCC separability. As a next step, we define the *minimal NCC depth*. Intuitively, the NCC depth of a given architecture is the minimal value  $L \in \mathbb{N}$ , for which there exists a neural network of depth  $L$  whose features are NCC separable. As we will show, the relationship between the effective depth of a neural network and the minimal NCC depth is tightly related with generalization.

**Definition 2** (Minimal NCC depth). *Suppose we have a dataset  $S = \bigcup_{c=1}^C S_c = \{(x_i, y_i)\}_{i=1}^m$  and a neural network architecture  $f^L = g^L \circ \dots \circ g^1$  with  $g^1 : \mathbb{R}^n \rightarrow \mathbb{R}^{n_0}$  and  $g^i \in \mathcal{G} \subset \{g' \mid g' : \mathbb{R}^{n_0} \rightarrow \mathbb{R}^{n_0}\}$  for all  $i = 2, \dots, L$ . The minimal NCC depth of the network is the minimal depth  $L$  for which there exist parameters  $W_f = \{W_i\}_{i=1}^L$  for which  $f_{W_f}^L = g_{W_L}^L \circ \dots \circ g_{W_1}^1$  perfectly fits the data using a NCC classifier. We denote the minimal NCC depth by  $d_{\min}(\mathcal{G}, S)$ .*

In this setting, we consider two balanced datasets  $S_1 = \{(x_i^1, y_i^1)\}_{i=1}^m$  and  $S_2 = \{(x_i^2, y_i^2)\}_{i=1}^m$ . We think of them as two splits of the training dataset  $S$ . We assume that the classifier  $h_{S_1}^{\gamma}$  is trained on  $S_1$  and fits  $> 99\%$  of its labels. We use  $S_2$  to evaluate the degree of generalization. We denote by  $X_j = \{x_i^j\}_{i=1}^m$  and  $Y_j = \{y_i^j\}_{i=1}^m$  the instances and labels in  $S_j$ .

As a technicality, throughout the analysis we make two main assumptions. The first is that the misclassified labels that  $h_{S_1}^{\gamma}$  produces on the set of samples  $X_2 = \bigcup_{c=1}^C \{x_{ci}^2\}_{i=1}^{m_0}$  are distributed uniformly.

**Definition 3** ( $\delta_m$ -uniform misclassification). *We say that the misclassification of a learning algorithm  $A : (S_1, \gamma) \mapsto h_{S_1}^{\gamma}$  is  $\delta_m$ -uniform, if with probability at least  $1 - \delta_m$  over the selection of  $S_1 = \{(x_i^1, y_i^1)\}_{i=1}^m$ ,  $S_2 = \{(x_i^2, y_i^2)\}_{i=1}^m \sim P_B(m)$ , the misclassification of  $h_{S_1}^{\gamma}$  over  $S_2$  is uniformly distributed (as a function of  $\gamma$ ).*

The above definition makes two assumptions regarding the learning algorithm. Namely, it assumes that with a high probability (over the selection of  $S_1, S_2$ ),  $h_{S_1}^{\gamma}$  makes a constant number of mistakes on  $S_2$  across all initializations  $\gamma$ . In addition, it assumes that the mistakes are distributed in a uniformly across the samples in  $S_2$  and their incorrect values are also distributed uniformly.

The second assumption is that: for any (large enough)  $m > 0$ ,

$$\mathbb{E}_{\tilde{Y}_2} [d_{\min}(\mathcal{G}, S_1 \cup \tilde{S}_2)] \leq \mathbb{E}_{\tilde{Y}_2} [d_{\min}(\mathcal{G}, S_1 \cup \tilde{S}_2)], \quad (4)$$

where  $\tilde{Y}_2 = \{\tilde{y}_i\}_{i=1}^m$  and  $\tilde{Y}_2 = \{\tilde{y}_i\}_{i=1}^m$  are uniformly selected to be sets  $Y = \{y_i\}_{i=1}^m$  that disagrees with  $\tilde{Y}_2$  on  $pm$  and  $qm$  values, where  $p \leq q$ . Informally, this assumption means that the expected minimal depth to fit  $(2 - p)m$  correct labels and  $pm$  labels is upper bounded by the expected minimal depth to fit  $(2 - q)m$  correct labels and  $qm$  random labels. Since in both cases the model has to fit at least  $m$  correct labels it should be sufficiently large to approximate the target function well. On the other hand, we typically need to progressively increase the capacity of the model in order to fit extended amounts of random labels. Finally, this assumption is empirically validated in Sec. 4.

Following the setting above, we are prepared to formulate our generalization bound.

**Proposition 1** (Comparative generalization). *Let  $m \in \mathbb{N}$  and  $p_m \in [0, 1]$ . Assume that the error of the learning algorithm is  $\delta_m$ -uniform. Assume that  $S_1, S_2 \sim P_B(m)$ . Let  $h_{S_1}^\gamma$  be the output of the learning algorithm given access to a dataset  $S_1$  and initialization  $\gamma$ . Then,*

$$\mathbb{E}_{S_1}[\text{err}_P(h_{S_1})] \leq \mathbb{P}_{S_1, S_2} \left[ \mathbb{E}_\gamma[\mathcal{d}_{S_1}(h_{S_1}^\gamma)] \geq \mathbb{E}_{\tilde{Y}_2}[\mathcal{d}_{\min}(\mathcal{G}, S_1 \cup \tilde{S}_2)] \right] + p_m + \delta_m, \quad (5)$$

where  $\tilde{Y}_2 = \{\tilde{y}_i\}_{i=1}^m$  is uniformly selected to be a set of labels that disagrees with  $Y_2$  on  $p_m m$  values.

The above proposition provides an upper bound on the expected test error of the classifier  $h_{S_1}^\gamma$  selected by the learning algorithm using a balanced dataset  $S_1$  of size  $m$ . To apply this bound we assume that the misclassification of the function  $h_{S_1}^\gamma$  on  $X_2$  is distributed uniformly (with probability at least  $1 - \delta_m$ ). As a penalty for the likelihood that this assumption fails, our bound includes the term  $\delta_m$ . To apply this bound, we need to choose a guess  $p_m \in [0, 1]$  of the expected error of  $h_{S_1}^\gamma$ .

The bound measures the probability (over the selection of  $S_1, S_2$ ) that  $\mathbb{E}_\gamma[\mathcal{d}_{S_1}(h_{S_1}^\gamma)]$  would be strictly smaller than  $\mathbb{E}_{\tilde{Y}_2}[\mathcal{d}_{\min}(\mathcal{G}, S_1 \cup \tilde{S}_2)]$ . Informally,  $\mathbb{E}_\gamma[\mathcal{d}_{S_1}(h_{S_1}^\gamma)]$  measures the expected effective depth of  $h_{S_1}^\gamma$  over the initialization and  $\mathbb{E}_{\tilde{Y}_2}[\mathcal{d}_{\min}(\mathcal{G}, S_1 \cup \tilde{S}_2)]$  measures the minimal depth required in order to fit a dataset of size  $2m$ , where  $(2 - p_m)m$  of the labels are correct and  $p_m m$  are random labels. In general, if  $h = e \circ f^L$  is a neural network of a fixed width  $n_0$ , it is impossible to fit an increasing amount of random labels without increasing  $L$ . Therefore, we expect  $\mathbb{E}_{\tilde{Y}_2}[\mathcal{d}_{\min}(\mathcal{G}, S_1 \cup \tilde{S}_2)]$  to tend to infinity as long as we take  $p_m m \rightarrow \infty$ . On the other hand,  $\mathbb{E}_\gamma[\mathcal{d}_{S_1}(h_{S_1}^\gamma)]$  should not increase at the same rate when  $m$  increases. Specifically, if  $p_m = 1/\sqrt{m}$ , we obtain that  $\mathbb{P} \left[ \mathbb{E}_\gamma[\mathcal{d}_{S_1}(h_{S_1}^\gamma)] \geq \mathbb{E}_{\tilde{Y}_2}[\mathcal{d}_{\min}(\mathcal{G}, S_1 \cup \tilde{S}_2)] \right] \xrightarrow{m \rightarrow \infty} 0$  and  $p_m \xrightarrow{m \rightarrow \infty} 0$ , giving us  $\mathbb{E}_{S_1}[\text{err}_P(h_{S_1})] \leq \delta_m + o_m(1)$ , which is small if the misclassification pattern of the learning algorithm is uniform with high likelihood.

Interestingly, if our minimal depth hypothesis holds, then  $\mathcal{d}_{S_1}(h_{S_1}^\gamma)$  is unaffected by the depth  $L$  of  $h_{S_1}^\gamma$  whenever  $L \geq L_0$ . Therefore, in this case, the generalization bound shows that as long as  $L \geq L_0$ , the test performance of  $h_{S_1}^\gamma$  should be unaffected by the choice of  $L$ .

We note that computing the first term in the bound is generally impossible, due to the limited access to training data. However, instead, we can empirically estimate this term using a set of  $k$  sampled pairs  $(S_1^i, S_2^i)$ , yielding an additional term that scales as  $\mathcal{O}(1/k)$  to be bound. This is provided in Prop. 2.

Finally, we note that the proposed generalization bound is fairly different from traditional generalization bounds [Vapnik, 1998, Shalev-Shwartz and Ben-David, 2014, Mohri et al., 2012]. Typically, the expected error is bounded by the sum between the train error and the ratio between the a measure of complexity of the selected hypothesis (e.g., depending on the number of parameters, their norm, etc') and  $\sqrt{m}$ . Furthermore, measuring the generalization using a traditional generalization bounds would still result in a vacuous bound even if an implicit depth minimization is evident. That is because, the overall number of parameters of the network after replacing the top, redundant, layers with a nearest class-center classifier would still exceed the number of training samples. On the other hand, the bound introduced in Prop. 1 takes a different form. In this case, we do not require that the size of the network would be small in comparison with  $\sqrt{m}$ , rather the bound guarantees generalization if the effective size of the network is *smaller* than networks that fit partially random labels. Therefore, even if the effective size of the network is larger than  $\sqrt{m}$ , our bound can still imply that the test error would be small.

## 4 Experiments

In this section we experimentally analyze the presence of neural collapse in the various layers of a trained network. In the first experiment, we validate the implicit bias of SGD to favor neural networks of minimal NCC depths. In the second experiment, we consider the effect of noisy labels on the extent of neural collapse, and specifically, on the minimal NCC depth. We show that NCC depth typically increases when extending the amount of noisy labels present in the data. For additional experiments see Appendix A.

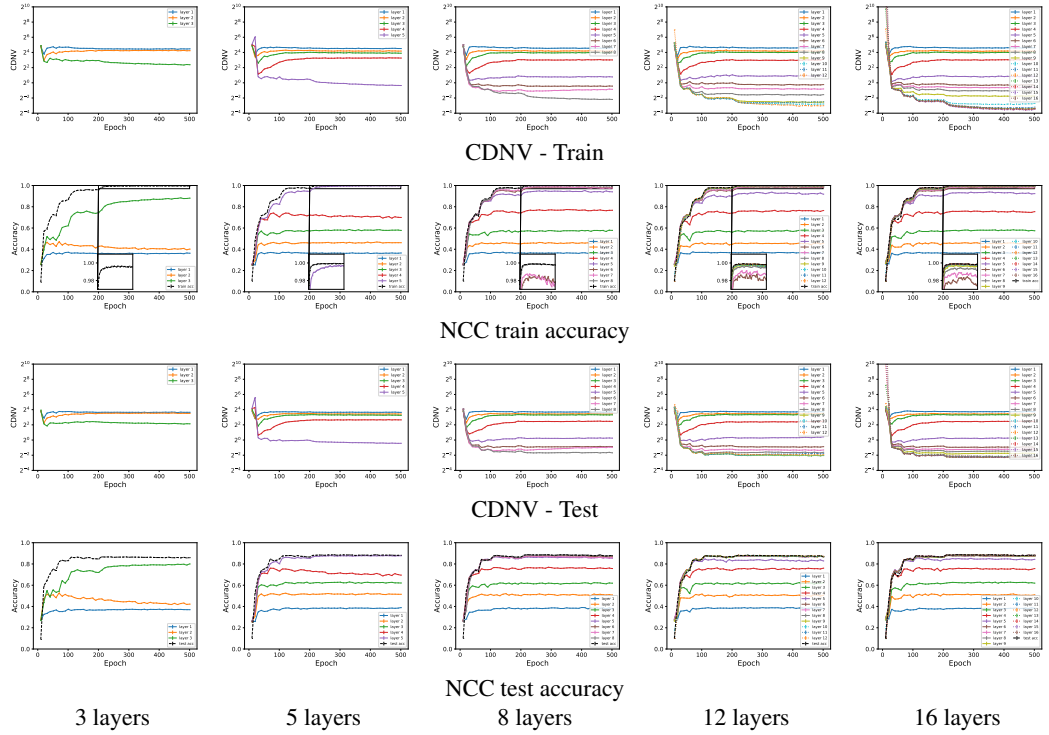


Figure 1: **Intermediate neural collapse with ConvNet-L-400 trained on CIFAR10.** In the first and second rows we plot the CDNV and the NCC accuracy rates of neural networks with varying numbers of hidden layers evaluated on the train data (plotted in lin-log scale). Each line stands for a different layer within the network. In the third and fourth rows we plot the same quantities over the test data.

#### 4.1 Setup

**Evaluation process.** Following our problem setup, we consider  $k$ -class classification problems (e.g., CIFAR10, STL10) and train a multilayered neural network  $h = e \circ f^L = e \circ g^L \circ \dots \circ g^1 : \mathbb{R}^n \rightarrow \mathbb{R}^C$  on some balanced training data  $S = \cup_{c=1}^C S_c = \cup_{c=1}^C \{(x_{ci}, y_{ci})\}_{i=1}^{m_0}$ . The model is trained using cross-entropy loss minimization between its logits and the one-hot encodings of the labels. Here,  $g^1, \dots, g^L$  are the various hidden layers of the network, where  $e$  is its top linear layer. As a second stage, the NCC accuracy of each sub-architecture  $f^i = g^i \circ \dots \circ g^1(x)$  ( $i \in [L]$ ) is evaluated as well. Throughout the experiments, we treat  $> 99\%$  fitting of the training data as a (close to) perfect interpolation of the data.

**Architectures and hyperparameters.** In this work we consider three types of architectures. The first architecture is a convolutional network (ConvNet), beginning with a stack of a  $2 \times 2$  convolutional layer with stride 2, batch normalization, a convolution of the same structure, batch normalization and ReLU. Following that we have a set of  $L$  stacks of  $3 \times 3$  convolutional layer with stride 1 and padding 1, batch normalization and ReLU. The output tensors of these layers shares the same shape as their input's shape. To effectively study the role of depth in neural networks, it makes sense to fix the width of each one of the layers. Therefore, we fix the number of channels in each convolutional layer to be  $H$ . The last layer is linear. The network is denoted by Conv- $L$ - $H$ . In the Appendix we also experiment with Multi-layered perceptrons and the standard ResNet-18 He et al. [2015].

The optimizations were carried out using SGD with batch size 128, learning rate scheduling with an initial learning rate 0.1, decayed three times by a factor of 0.1 at epochs 60, 120, and 160, momentum 0.9 and weight decay  $5e-4$ . Each model is trained for 500 epochs.

**Datasets.** Throughout the experiments, we consider three different datasets: (i) MNIST; (ii) Fashion MNIST and (iii) CIFAR10. For CIFAR10 we used random cropping, random horizontal flips and

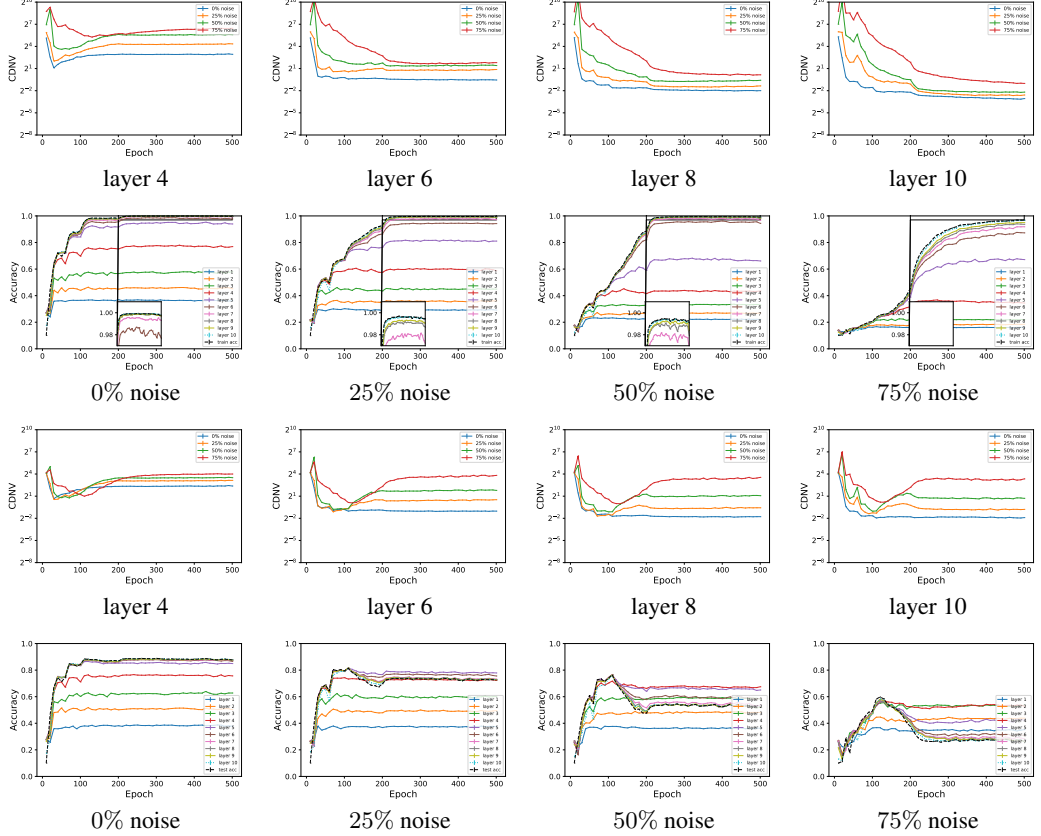


**Figure 2: Intermediate neural collapse with ConvNet-10-500 trained on CIFAR10 with noisy labels.** In the first row we plot the CDNV on the train data for layers 4, 6, 8, 10 of networks trained with varying ratios of label noise (see legend). In the second row each figures reports the NCC accuracy rates of the various layers of a network trained with a certain amount of noisy labels (see titles). In the third and fourth rows we report the same experiments, but for the test data.

random rotations (by  $15k$  degrees for  $k$  uniformly sampled from [24]). For all datasets we standardized the data.

## 4.2 Results

**Minimal depth in neural networks.** To study the bias towards minimal depth, we trained a set of neural networks with varying depths. In Fig. 1 we plot the results of this experiment, for ConvNet- $L$ -400 networks. In each row we consider a different evaluation metric (the CDNV on the train and test data and the NCC classification accuracy on the train and test data) and in each column, we consider a neural network of a different depth  $L$ . The  $i$ 'th line stands for the CDNV at train time of the  $i$ 'th hidden layer of the neural network. As can be seen, the networks with 8 or higher hidden layers, the eighth and higher layers have NCC train accuracy  $\approx 100\%$ . Therefore, these networks are effectively of depth 7. In addition, we observe that in general, neural collapse strengthens when increasing the depth of the neural network, on both train and test data. For instance, even though a 3 hidden layers network perfectly fits the training data without neural collapse, we observe neural collapse with deeper networks.

**Neural collapse with random labels.** Informally, Prop. 1 shows that the error of a trained model  $h_{S_1}$  is upper bounded by  $p$  if its effective depth is smaller than the minimal depth for fitting a dataset with  $pm/2$  ratio of incorrect labels. To validate that this is indeed the case, we follow Mixon et al. [2020] and investigate the emergence of neural collapse in the presence of random labels. In Mixon et al. [2020] they showed the neural collapse tends to happen on the training data even in the case when 100% of the training labels are selected uniformly at random from  $[C]$ . In this experiment we

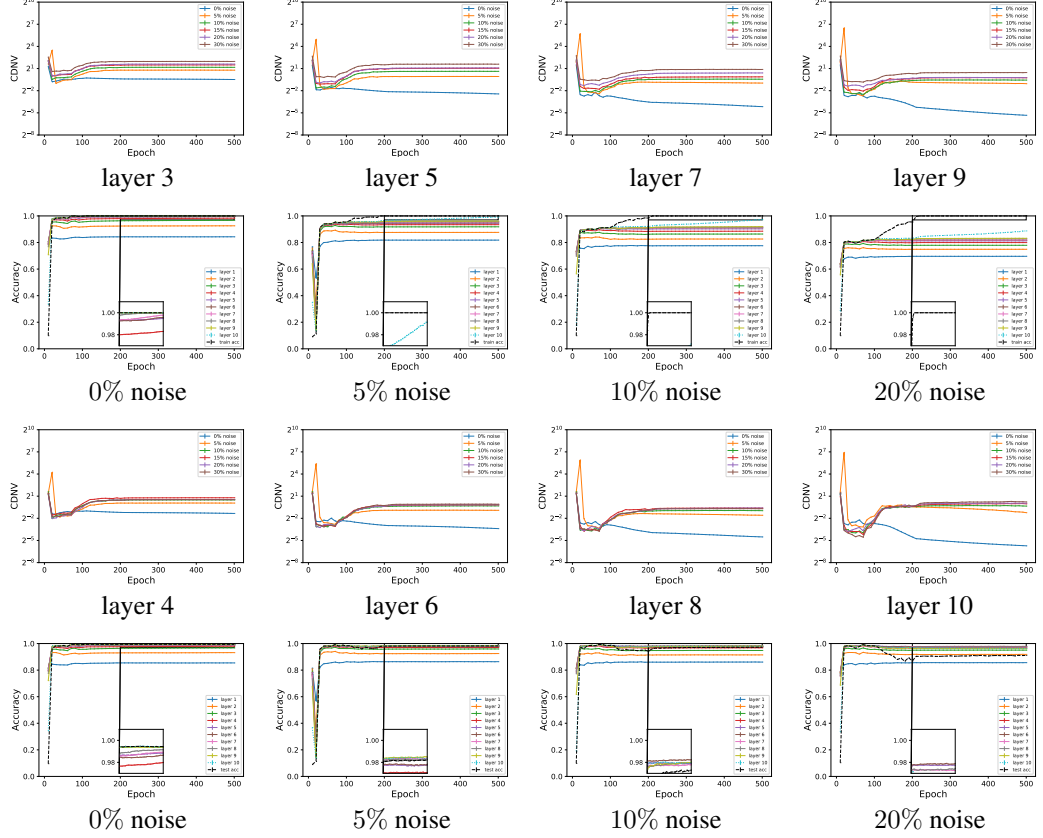


Figure 3: **Intermediate neural collapse with ConvNet-10-50 trained on MNIST with noisy labels.** In the first row we plot the CDNV on the train data for layers 3, 5, 7, 9 of networks trained with varying ratios of label noise (see legend). In the second row each figures reports the NCC accuracy rates of the various layers of a network trained with a certain amount of noisy labels (see titles). In the third and fourth rows we report the same experiments, but for the test data.

intend to compare the *degree* of collapse in the various layers of a neural network that is being trained with different portions of random labels.

We train ConvNet-10-500 for CIFAR10 classification with 0%, 25%, 50% and 75% of the labels being replaced with random labels. We compare the degree of redundancy of the various layers of the networks as a function of the amount of noise in the data. The results are summarized in Fig. 2. In the first row we plot the CDNV of the  $i$ th layer of the various models on the train data for different layers in the networks, with  $i = 4, 6, 8, 10$ . In the second row we plot the NCC accuracy rates of the various layers of the models, when trained with different amounts of random labels. We also compare the performance with the train accuracy rate of the full model. In the third and fourth rows we plot exactly the same as the first two rows, but for the test data.

As can be seen in Fig. 2, we get some degree of neural collapse (on the training data) when training with or without noisy labels. However, we observe several distinctions between the two settings. First, when training without noisy labels, we obtain a higher degree of neural collapse on each one of the layers. In addition, when training with 25% noisy labels, the seventh layer's NCC accuracy rate is lower than 98%, in contrast to training without noisy labels which achieve  $\approx 100\%$  accuracy.

In Fig. 3 we repeat the experiment with ConvNet-10-50 trained on MNIST with 0%, 5%, 10% and 20% noisy labels. First, we observe that in each case the model perfectly fits the train labels. On the other hand, the degree of neural collapse on the train data does distinguish between the two training regimes (with/without noisy labels). For instance, the CDNV on the train (and test) data is significantly lower across all layers when training without noisy labels. In addition, when training without noisy labels, the NCC accuracy rates of the 5 top-most layers is greater than 99%. In contrast,

when training with 5% noisy labels, only the tenth layer achieves an NCC train accuracy that exceeds 99%. Therefore, the effective NCC depth of a network trained without noisy labels is much smaller than the effective NCC depth of a network trained with at least 5% noisy labels.

Interestingly, we also observe that NCC classifiers corresponding to intermediate layers are relatively resilient to noisy labels. Namely, we observe in Figs. 2 and 3 (fourth row) that when training a model with noisy labels, the NCC classifiers corresponding to intermediate layers achieve better test performance than the model itself.

## 5 Conclusions

Training deep neural networks is a successful approach for a variety of learning problems. However, the role of depth in deep learning and the functionalities learned by each layer are not very clear. In this paper we presented a new perspective on this problem by studying the emergence of neural collapse in the intermediate layers during training.

While Papyan et al. [2020] suggested that neural collapse is a property that emerges in the penultimate layer of an overparameterized neural network at the stage where perfect fitting of the data is achieved, we suggest several extensions to this observation.

First, we show that neural collapse improves when increasing the depth of a network. In addition, we empirically showed that the within-class variance collapse and NCC separability tend to emerge within the intermediate layers of a neural network and not just in the penultimate layer. Following this observation, we define the effective NCC depth of a neural network that measures the minimal layer at which the data becomes NCC separable. We hypothesize and empirically validate that the effective NCC depth of networks do not grow with the depth of the network.

## Acknowledgements

This work was supported by the Center for Brains, Minds and Machines (CBMM), funded by NSF STC award CCF – 1231216.

The authors would like to thank Tomaso Poggio, András György, Lior Wolf, Andrzej Banburski, Ido Ben-Shaul and X. Y. Han for illuminating discussions during the preparation of this manuscript.

## References

K. Arulkumaran, A. Cully, and J. Togelius. Alphastar: An evolutionary computation perspective, 2019. URL <http://arxiv.org/abs/1902.01724>. cite arxiv:1902.01724.

I. Ben-Shaul and S. Dekel. Nearest class-center simplification through intermediate layers. *CoRR*, abs/2201.08924, 2022. URL <https://arxiv.org/abs/2201.08924>.

T. Brown, B. Mann, N. Ryder, M. Subbiah, J. D. Kaplan, P. Dhariwal, A. Neelakantan, P. Shyam, G. Sastry, A. Askell, S. Agarwal, A. Herbert-Voss, G. Krueger, T. Henighan, R. Child, A. Ramesh, D. Ziegler, J. Wu, C. Winter, C. Hesse, M. Chen, E. Sigler, M. Litwin, S. Gray, B. Chess, J. Clark, C. Berner, S. McCandlish, A. Radford, I. Sutskever, and D. Amodei. Language models are few-shot learners. In *Advances in Neural Information Processing Systems*, volume 33, pages 1877–1901. Curran Associates, Inc., 2020.

M. Chen, J. Tworek, H. Jun, Q. Yuan, H. P. de Oliveira Pinto, J. Kaplan, H. Edwards, Y. Burda, N. Joseph, G. Brockman, A. Ray, R. Puri, G. Krueger, M. Petrov, H. Khlaaf, G. Sastry, P. Mishkin, B. Chan, S. Gray, N. Ryder, M. Pavlov, A. Power, L. Kaiser, M. Bavarian, C. Winter, P. Tillet, F. P. Such, D. Cummings, M. Plappert, F. Chantzis, E. Barnes, A. Herbert-Voss, W. H. Guss, A. Nichol, A. Paino, N. Tezak, J. Tang, I. Babuschkin, S. Balaji, S. Jain, W. Saunders, C. Hesse, A. N. Carr, J. Leike, J. Achiam, V. Misra, E. Morikawa, A. Radford, M. Knight, M. Brundage, M. Murati, K. Mayer, P. Welinder, B. McGrew, D. Amodei, S. McCandlish, I. Sutskever, and W. Zaremba. Evaluating large language models trained on code, 2021.

J. Devlin, M.-W. Chang, K. Lee, and K. Toutanova. BERT: Pre-training of deep bidirectional transformers for language understanding. In *Proceedings of the 2019 Conference of the North American Chapter of the Association for Computational Linguistics: Human Language Technologies, Volume 1 (Long and Short Papers)*. Association for Computational Linguistics, jun 2019.

R. Eldan and O. Shamir. The power of depth for feedforward neural networks, 2016.

T. Galanti, A. György, and M. Hutter. On the role of neural collapse in transfer learning. In *International Conference on Learning Representations*, 2022. URL <https://openreview.net/forum?id=SwIp410B6aQ>.

K. He, X. Zhang, S. Ren, and J. Sun. Deep residual learning for image recognition. In *2016 IEEE Conference on Computer Vision and Pattern Recognition (CVPR)*, pages 770–778, 2016. doi: 10.1109/CVPR.2016.90.

K. He et al. Delving deep into rectifiers: Surpassing human-level performance on imagenet. In *ICCV*, 2015.

A. Jacot, F. Gabriel, and C. Hongler. Neural tangent kernel: Convergence and generalization in neural networks. In *Proceedings of the 32nd International Conference on Neural Information Processing Systems*, NIPS, page 8580–8589, Red Hook, NY, USA, 2018. Curran Associates Inc.

A. Jacot, F. Gabriel, and C. Hongler. Freeze and chaos for dnns: an ntk view of batch normalization, checkerboard and boundary effects. *CoRR*, abs/1907.05715, 2019. URL <http://arxiv.org/abs/1907.05715>.

J. Lee, L. Xiao, S. Schoenholz, Y. Bahri, R. Novak, J. Sohl-Dickstein, and J. Pennington. Wide neural networks of any depth evolve as linear models under gradient descent. In *Advances in Neural Information Processing Systems 32*, pages 8572–8583. Curran Associates, Inc., 2019.

D. G. Mixon, H. Parshall, and J. Pi. Neural collapse with unconstrained features, 2020.

M. Mohri, A. Rostamizadeh, and A. Talwalkar. *Foundations of Machine Learning*. The MIT Press, 2012. ISBN 026201825X.

V. Papyan, X. Y. Han, and D. L. Donoho. Prevalence of neural collapse during the terminal phase of deep learning training. *Proceedings of the National Academy of Sciences*, 117(40):24652–24663, 2020.

T. Poggio, A. Banburski, and Q. Liao. Theoretical issues in deep networks. *Proceedings of the National Academy of Sciences*, 2020.

I. Safran, R. Eldan, and O. Shamir. Depth separations in neural networks: What is actually being separated?, 2021.

S. Shalev-Shwartz and S. Ben-David. *Understanding Machine Learning - From Theory to Algorithms*. Cambridge University Press, 2014. ISBN 978-1-10-705713-5.

D. Silver, A. Huang, C. J. Maddison, A. Guez, L. Sifre, G. van den Driessche, J. Schrittwieser, I. Antonoglou, V. Panneershelvam, M. Lanctot, S. Dieleman, D. Grewe, J. Nham, N. Kalchbrenner, I. Sutskever, T. Lillicrap, M. Leach, K. Kavukcuoglu, T. Graepel, and D. Hassabis. Mastering the game of Go with deep neural networks and tree search. *Nature*, 529:484–489, 2016. ISSN 0028-0836. doi: 10.1038/nature16961.

Y. Taigman, M. Yang, M. Ranzato, and L. Wolf. Deepface: Closing the gap to human-level performance in face verification. In *Conference on Computer Vision and Pattern Recognition (CVPR)*, 2014.

V. N. Vapnik. *Statistical Learning Theory*. Wiley-Interscience, 1998.

H. Wang, S. Ma, L. Dong, S. Huang, D. Zhang, and F. Wei. Deepnet: Scaling transformers to 1,000 layers. *arXiv preprint arXiv:2203.00555*, 2022.

X. Zhai, A. Kolesnikov, N. Houlsby, and L. Beyer. Scaling vision transformers, 2021.

## A Additional Experiments

In this section we provide some additional experiments. Throughout the experiments we use the Conv- $L$ - $H$  architecture proposed in the main text, Multi-layered perceptrons and ResNet-18 He et al. [2016]. Our MLPs, denoted by MLP- $L$ - $H$  consist of  $L$  hidden layers, where each layer consists of a linear layer of width  $H$ , followed by batch normalization and ReLU. On top of that we compose a linear output layer.

**Auxiliary experiments on the effective depth.** We repeated the experiment in Fig. 1. In Figs. 4, 5 and 6 we plot the results of the same experiment, with different networks and datasets (see captions). As can be seen, the observations collected in the main text are reproduced.

**Auxiliary experiments with noisy labels.** We repeated the experiment in Figs. 2 and 3. In Figs. 7 and 8 we plot the results of the same experiment, with different networks and datasets (see captions). As can be seen, the observations collected in the main text are reproduced.

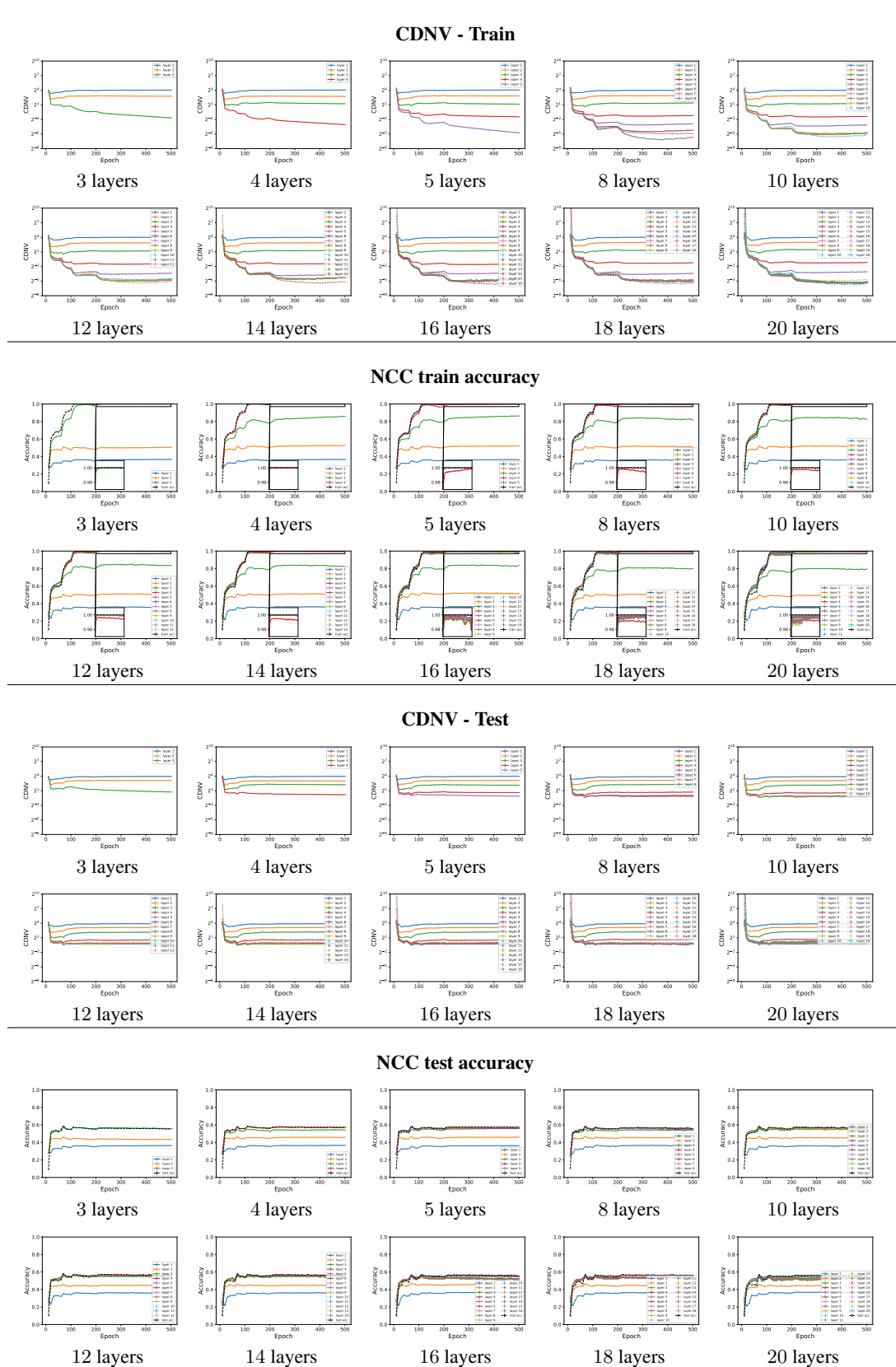


Figure 4: **Intermediate neural collapse with MLP-L-300 trained on CIFAR10.** See Fig. 1 for details.

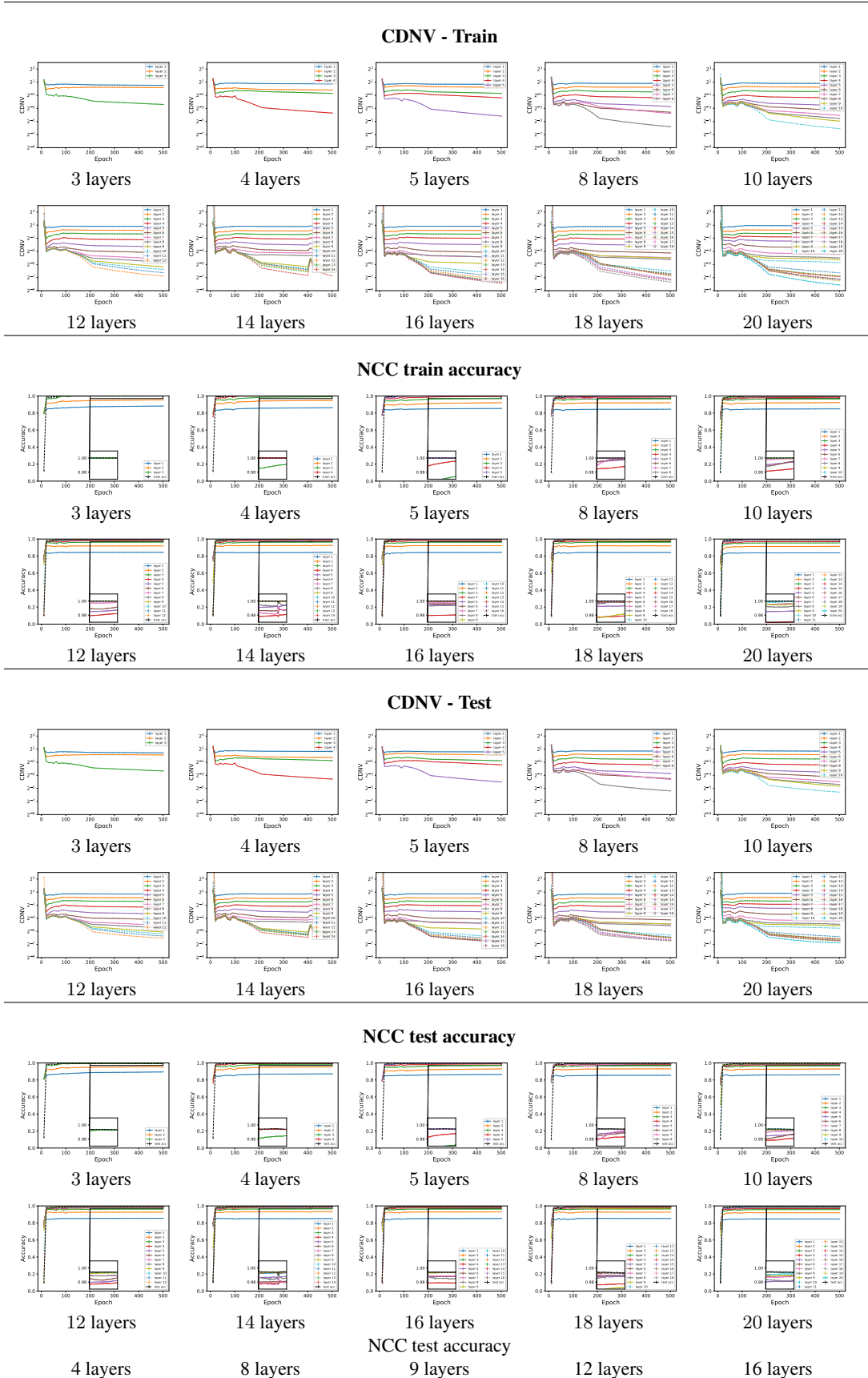


Figure 5: **Intermediate neural collapse with ConvNet-L-50 trained on MNIST.** See Fig. 1 for details.

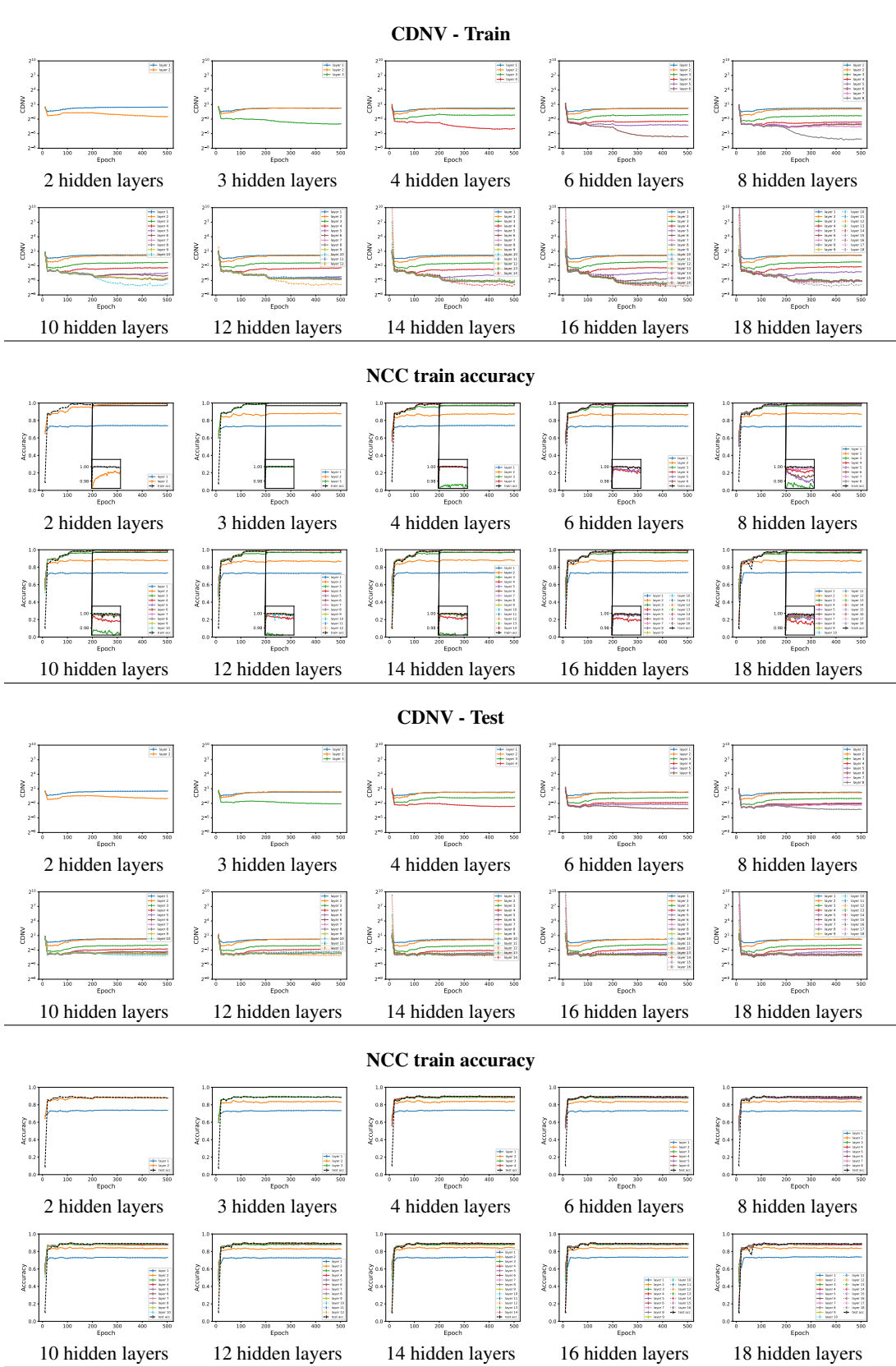


Figure 6: **Intermediate neural collapse with MLP-L-100 trained on Fashion MNIST.** See Fig. 1 for details.

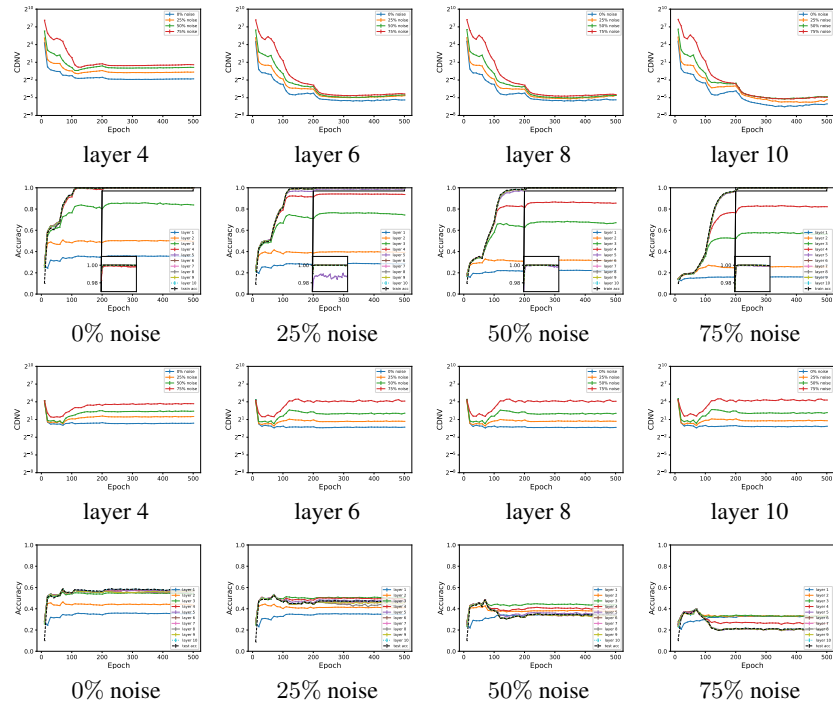


Figure 7: **Intermediate neural collapse with MLP-10-500 trained on CIFAR10 with noisy labels.**  
See Fig. 2 for details.

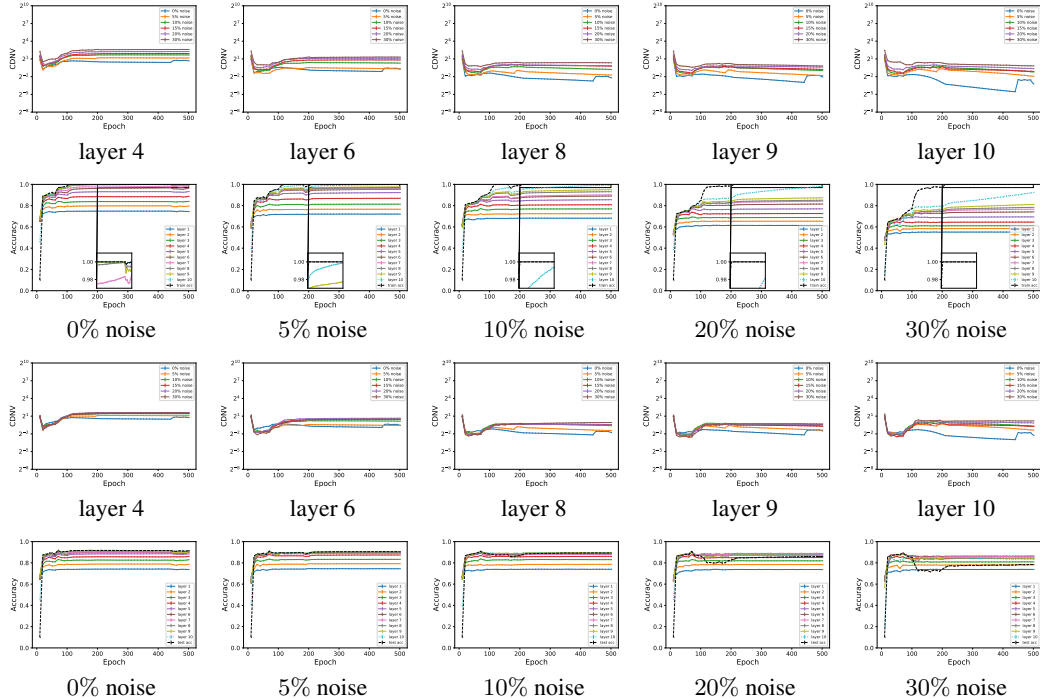


Figure 8: **Intermediate neural collapse with Conv-10-100 trained on Fashion MNIST with noisy labels.**  
See Fig. 2 for details.

## B Proofs

**Proposition 1** (Comparative generalization). *Let  $m \in \mathbb{N}$  and  $p_m \in [0, 1]$ . Assume that the error of the learning algorithm is  $\delta_m$ -uniform. Assume that  $S_1, S_2 \sim P_B(m)$ . Let  $h_{S_1}^\gamma$  be the output of the learning algorithm given access to a dataset  $S_1$  and initialization  $\gamma$ . Then,*

$$\mathbb{E}_{S_1}[\text{err}_P(h_{S_1})] \leq \mathbb{P}_{S_1, S_2} \left[ \mathbb{E}_\gamma[\ell_{S_1}(h_{S_1}^\gamma)] \geq \mathbb{E}_{\tilde{Y}_2}[\ell_{\min}(\mathcal{G}, S_1 \cup \tilde{S}_2)] \right] + p_m + \delta_m, \quad (5)$$

where  $\tilde{Y}_2 = \{\tilde{y}_i\}_{i=1}^m$  is uniformly selected to be a set of labels that disagrees with  $Y_2$  on  $p_m m$  values.

*Proof.* Let  $S_1 = \{(x_i^1, y_i^1)\}_{i=1}^m$  and  $S_2 = \{(x_i^2, y_i^2)\}_{i=1}^m$  be two balanced datasets. Let  $\tilde{Y}_2$  be an  $\epsilon$ -balanced set of labels that disagrees with  $Y_2$  on at least  $p$  labels. We define four different events:

$$\begin{aligned} A_1 &= \{S_1, S_2 \mid \text{the mistakes of } h_{S_1}^\gamma \text{ are not uniform over } S_2\} \\ A_2 &= \{S_1, S_2 \mid (S_1, S_2) \notin A_1 \text{ and } \mathbb{E}_\gamma[\ell_{S_1}(h_{S_1}^\gamma)] < \mathbb{E}_{\tilde{Y}_2}[\ell_{\min}(\mathcal{F}, S_1 \cup \tilde{S}_2)]\} \\ A_3 &= \{S_1, S_2 \mid (S_1, S_2) \notin A_1 \text{ and } \mathbb{E}_\gamma[\ell_{S_1}(h_{S_1}^\gamma)] \geq \mathbb{E}_{\tilde{Y}_2}[\ell_{\min}(\mathcal{F}, S_1 \cup \tilde{S}_2)]\} \\ B_1 &= \{S_1, S_2 \mid \mathbb{E}_\gamma[\ell_{S_1}(h_{S_1}^\gamma)] \geq \mathbb{E}_{\tilde{Y}_2}[\ell_{\min}(\mathcal{F}, S_1 \cup \tilde{S}_2)]\} \end{aligned} \quad (6)$$

By the law of total expectation

$$\begin{aligned} \mathbb{E}_{S_1}[\text{err}_P(h_{S_1})] &= \mathbb{E}_{S_1, S_2}[\text{err}_{S_2}(h_{S_1})] \\ &= \sum_{i=1}^3 \mathbb{P}[A_i] \cdot \mathbb{E}_{S_1, S_2}[\text{err}_{S_2}(h_{S_1}) \mid A_i] \\ &\leq \mathbb{P}[A_1] + \mathbb{E}_{S_1, S_2}[\text{err}_{S_2}(h_{S_1}) \mid A_2] + \mathbb{P}[B_1], \end{aligned} \quad (7)$$

where the last inequality follows from  $\text{err}_{S_2}(h_{S_1}) \leq 1$ ,  $\mathbb{P}[A_2] \leq 1$  and  $A_3 \subset B_1$ .

Assume that  $(S_1, S_2) \in A_2$ . Then, the misclassifications of  $h_{S_1}^\gamma$  over  $S_2$  is uniformly distributed (with respect to the selection of  $\gamma$ ). Assume by contradiction that  $\text{err}_{S_2}(h_{S_1}^\gamma) \geq p$  for some initialization  $\gamma$ . Then, since misclassifications of  $h_{S_1}^\gamma$  over  $S_2$  is uniformly distributed,  $\text{err}_{S_2}(h_{S_1}^\gamma) \geq p$  for all initializations  $\gamma$ . Therefore, we have  $\mathbb{E}_{\tilde{Y}_2}[\ell_{\min}(\mathcal{F}, S_1 \cup \tilde{S}_2)] \leq \mathbb{E}_\gamma[\ell_{S_1}(h_{S_1}^\gamma)] < \mathbb{E}_{\tilde{Y}_2}[\ell_{\min}(\mathcal{F}, S_1 \cup \tilde{S}_2)]$  in contradiction to Eq. 4. Therefore, we conclude that in this case,  $\mathbb{E}_\gamma[\text{err}_{S_2}(h_{S_1}^\gamma)] \leq p$  and  $\mathbb{E}_{S_1, S_2}[\text{err}_{S_2}(h_{S_1}) \mid A_2] \leq p$ . In addition, since the learning algorithm enjoys  $\delta_m$ -uniform misclassification,  $\mathbb{P}[A_1] \leq \delta_m$ .  $\square$

**Proposition 2.** *Let  $m \in \mathbb{N}$  and  $p_m \in [0, 1]$ . Assume that the error of the learning algorithm is  $\delta_m$ -uniform. Assume that  $S_1, S_2, S_1^i, S_2^i \sim P_B(m)$ . Let  $h_{S_1}^\gamma$  be the output of the learning algorithm given access to a dataset  $S_1$  and initialization  $\gamma$ . Then, with probability at least  $1 - \delta$  over the selection of  $\{(S_1^i, S_2^i)\}_{i=1}^k$ , we have*

$$\mathbb{E}_{S_1}[\text{err}_P(h_{S_1})] \leq \frac{1}{k} \sum_{i=1}^k \mathbb{E}_\gamma[\ell_{S_1^i}(h_{S_1}^\gamma)] \geq \mathbb{E}_{\tilde{Y}_2^i}[\ell_{\min}(\mathcal{G}, S_1^i \cup \tilde{S}_2^i)] + p_m + \delta_m + \sqrt{\frac{\log(2/\delta)}{2k}},$$

where  $\tilde{Y}_2^i = \{\tilde{y}_i\}_{i=1}^m$  is uniformly selected to be a set of labels that disagrees with  $Y_2^i$  on  $p_m m$  values.

*Proof.* By Prop. 1, we have

$$\mathbb{E}_{S_1}[\text{err}_P(h_{S_1})] \leq \mathbb{P}_{S_1, S_2} \left[ \mathbb{E}_\gamma[\ell_{S_1}(h_{S_1}^\gamma)] \geq \mathbb{E}_{\tilde{Y}_2}[\ell_{\min}(\mathcal{G}, S_1 \cup \tilde{S}_2)] \right] + p_m + \delta_m \quad (8)$$

We define i.i.d. random variables

$$V_i = \mathbb{I} \left[ \mathbb{E}_\gamma[\ell_{S_1^i}(h_{S_1}^\gamma)] \geq \mathbb{E}_{\tilde{Y}_2^i}[\ell_{\min}(\mathcal{G}, S_1^i \cup \tilde{S}_2^i)] \right]. \quad (9)$$

Therefore, we can rewrite,

$$\mathbb{P}_{S_1, S_2} \left[ \mathbb{E}_\gamma[\ell_{S_1}(h_{S_1}^\gamma)] \geq \mathbb{E}_{\tilde{Y}_2}[\ell_{\min}(\mathcal{G}, S_1 \cup \tilde{S}_2)] \right] = \mathbb{E}[V_1] \quad (10)$$

By Hoeffding's inequality,

$$\Pr \left[ \left| k^{-1} \sum_{i=1}^k V_i - \mathbb{E}[V_1] \right| \geq \epsilon \right] \leq 2 \exp(-2k\epsilon^2). \quad (11)$$

By choosing  $\epsilon = \sqrt{\log(1/2\delta)/2k}$ , we obtain that with probability at least  $1 - \delta$ , we have

$$\mathbb{E}[V_1] \leq \frac{1}{k} \sum_{i=1}^k V_i + \sqrt{\log(1/2\delta)/2k}. \quad (12)$$

When combined with Eq. 5, we obtain the desired bound.  $\square$